AIP | Journal of Applied Physics

Effect of ternary mixed crystals on interface optical phonons in wurtizte InxGa1−xN/GaN quantum wells

Wen-Deng Huang, Guang-De Chen, and Ya-Jie Ren

Citation: J. Appl. Phys. **112**, 053704 (2012); doi: 10.1063/1.4748173
View online: http://dx.doi.org/10.1063/1.4748173
View Table of Contents: http://jap.aip.org/resource/1/JAPIAU/v112/i5
Published by the American Institute of Physics.

Effect of ternary mixed crystals on interface optical phonons in wurtizte $In_xGa_{1-x}N$/GaN quantum wells

Wen-Deng Huang,[1,2,a)] Guang-De Chen,[1] and Ya-Jie Ren[2]
[1]*MOE Key Laboratory for Nonequilibrium Synthesis and Modulation of Condensed Matter, School of Science, Xi'an Jiaotong University, Xi'an 710049, China*
[2]*Department of Physics, Shaanxi University of Technology, Hanzhong 723001, China*

(Received 26 May 2012; accepted 20 July 2012; published online 5 September 2012)

The effect of ternary mixed crystals on the interface optical phonons in wurtizte $In_xGa_{1-x}N$/GaN quantum wells is studied based on the modified random-element isodisplacement model and dielectric continuum model. The results show that the interface optical phonons appear different frequency range with different indium concentration. The frequencies of interface optical phonons in the high frequency range decrease almost linearly with increasing indium concentration and do not vary almost linearly in the low frequency range. The indium concentration has more important effect on the electron-phonon interaction in low frequency range. © *2012 American Institute of Physics*. [http://dx.doi.org/10.1063/1.4748173]

I. INTRODUCTION

The ternary and quaternary, and even multinary III-nitride mixed crystals, offer flexible choices for consecutive layers in heterostructures and quantum wells with desirable lattice constants and band offsets, which makes an important potential application of III-nitrides in LEDs and LDs with wavelengths from red to deep ultraviolet.[1–3] The optical phonons and carrier-phonon interactions play an important role in many of the optoelectronic properties and have been studied intensively by many authors. Romanov *et al.*[4] have investigated polar interface vibrations in AlN/GaN quantum dots. Komirenko *et al.*[5] have investigated dispersion of polar optical phonons in symmetrical wurtzite AlN/GaN and $Al_{0.15}Ga_{0.85}N$/GaN quantum wells. The group of Lee[6] have studied the confined optical phonon modes and scattering in wurtzite crystals and double heterostructures systems. Gleize *et al.*[7] have analyzed the anisotropy effects on the polar optical phonons in wurtzite AlN/GaN single QWs and super-lattices. Shi[8] has investigated the interface phonons in AlN/GaN multiple QWs. Shi and Chu[9] have also studied the propagating phonons in $Al_{0.15}Ga_{0.85}N$/GaN multiple QWs. Lü and Cao[10] have investigated confined optical phonon modes in wurtzite GaN/ZnO quantum wells. Wei *et al.*[11] have investigated the interface optical phonon modes in wurtzite GaN/ZnO quantum wells. More recently, Zhou and Xie[12] have studied the electron-interface optical phonon interactions in rectangular wire and quantum dot. However, to the best our knowledge, most of the theoretical work published so far study on binary nitride, the effect of mixed crystals on the optical phonons and electron-phonon interactions in quantum well composed of ternary and quaternary, and even multinary, III-nitride crystals have not been fully studied. In the present paper, we will investigate the effect of ternary mixed crystals on the interface optical phonon in $In_xGa_{1-x}N$/GaN quantum wells.

The paper is organized as follows. In Sec. II, basic equations to describe the polar optical phonons in bulk wurtzite ternary mixed crystals are outlined for self-sufficiency. The IO phonon modes and electron-IO phonon interactions in wurtzite $In_xGa_{1-x}N$/GaN QWs are solved. The numerical results for the effect of ternary mixed crystals on the dispersions and electron-phonon interactions of IO phonons in $In_xGa_{1-x}N$/GaN QWs are given and discussed in Sec. III. Finally, the main conclusions are summarized in Sec. IV.

II. THEORY

A. The optical phonons in wurtzite ternary mixed crystals

By using the modified random-element isodisplacement model,[13] the frequencies of A_1(LO), A_1(TO), E_1(LO), and E_1(TO) in the wurtzite ternary mixed crystals $A_xB_{1-x}C$ are obtained by the following routes:

$$\omega_{Xi}^2 = \frac{\Omega_{Xbi}^2 + \Omega_{Xai}^2}{2} \pm \left[\left(\frac{\Omega_{Xbi}^2 - \Omega_{Xai}^2}{2} \right)^2 + x(1-x)\Omega_{Xbai}^4 \right]^{1/2}, \tag{1}$$

$$\Omega_{Xbi}^2 = \omega_{bi}^2 + (1-x)\alpha_{Xi}\omega_{bi'}^2, \tag{2}$$

$$\Omega_{Xai}^2 = \omega_{ai}^2 + x_{Xi}\omega_{ai'}^2, \tag{3}$$

$$\Omega_{Xbai}^4 = \left[\left(\frac{\delta_{bi}}{\delta_{ai}} \right)^{1/2} \beta_{Xi}\omega_{bi'}\omega_{ai'} + \frac{\bar{\mu}}{m_C}\omega_{Ai}^2 \right] \times \left[\left(\frac{\delta_{ai}}{\delta_{bi}} \right)^{1/2} \beta_{Xi}\omega_{bi'}\omega_{ai'} + \frac{\bar{\mu}}{m_C}\omega_{Bi}^2 \right], \tag{4}$$

$$\beta_{Ti} = -\gamma_i, \quad \beta_{Li} = (3-\gamma_i)/\varepsilon_{\infty i}, \tag{5}$$

$$\bar{\mu} = \sqrt{\mu_a \mu_b}, \tag{6}$$

where the subscript $a(b)$ stands for binary crystal AC (BC), the subscript i stands for z- and ⊥(x-y plane) polarization

a)Author to whom correspondence should be addressed. Fax: +86 0916 2641930. E-mail: sxlgwendeng@163.com.

directions, X stands for longitudinal optical (LO) and transverse optical (TO) components. $\mu_a(\mu_b)$ is the reduced mass of binary crystal AC (BC). γ_i is a introduced parameter, we take $\gamma_z = 1 - 0.1 \times (3/4\pi)$ and $\gamma_\perp = 1 + 0.2 \times (3/4\pi)$.[13] The high-frequency dielectric constant in ternary mixed crystal $A_xB_{1-x}C$ is

$$\frac{\varepsilon_{\infty i} - 1}{3 + \gamma_i(\varepsilon_{\infty i} - 1)} = x\frac{v_a}{v}\frac{\varepsilon_{\infty ai} - 1}{3 + \gamma_i(\varepsilon_{\infty ai} - 1)} + (1 - x)\frac{\varepsilon_{\infty bi} - 1}{3 + \gamma_i(\varepsilon_{\infty bi} - 1)}, \quad (7)$$

where v is the volume of the unit cell of mixed crystal, v_a and v_b are the unit cell volumes of binary crystal AC and CB. The other quantities are given by

$$\omega_{ai}^2 = \omega_{ai}^2\left(1 - (1 - x)\frac{u_a}{m_C}\right), \quad (8)$$

$$\omega_{ai'}^2 = \left[\delta_{ai}\frac{v_a}{v}\frac{3 + \gamma_i(\varepsilon_{\infty i} - 1)}{\gamma_i(3 + \gamma_i(\varepsilon_{\infty ai} - 1)}(\omega_{Ai}^2 - \omega_{Tai}^2)\right], \quad (9)$$

$$\omega_{Ai}^2 = \frac{3 + (\varepsilon_{\infty ai} - 1)}{3 + \gamma_i(\varepsilon_{\infty ai} - 1)}\omega_{Tai}^2, \quad (10)$$

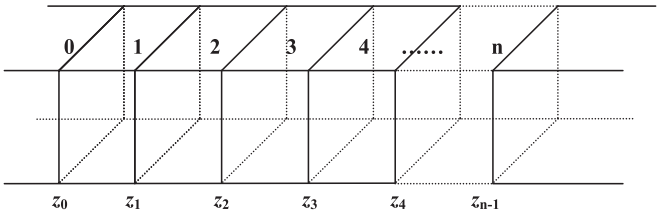

FIG. 1. A general multilayer Q2D wurtzite heterostructures.

$$\delta_{ai} = 1 - x\frac{u_a}{m_C}\left(1 - \frac{e_{bi}}{e_{ai}}\right). \quad (11)$$

The other variables $\omega_{bi}, \omega'_{bi}$, ω_{Bi}, and δ_{ai} can be obtained by interchanging a by b and x by $1 - x$.

B. The interface optical phonons in wurtizte quantum wells

We consider a wurtzite symmetry multilayer heterostructures (Fig. 1). Using the using the determinate method based on the DC model, the dispersion relation of interface optical phonon modes can be obtained by the below $2n \times 2n$ determinant

$$\begin{vmatrix}
a_0 & b_1 & b'_1 & 0 & 0 & 0 & 0 & 0 & 0 & 0 & 0 & 0 & 0 & 0 & 0 & 0 \\
a'_0 & c_1 & c'_1 & 0 & 0 & 0 & 0 & 0 & 0 & 0 & 0 & 0 & 0 & 0 & 0 & 0 \\
0 & a_1 & a_1 & b_2 & b'_2 & \cdots & 0 & 0 & 0 & 0 & 0 & 0 & 0 & 0 & 0 & 0 \\
0 & a'_1 & -a'_1 & c_2 & c'_2 & \cdots & 0 & 0 & 0 & 0 & 0 & 0 & 0 & 0 & 0 & 0 \\
0 & 0 & 0 & a_2 & a_2 & \cdots & 0 & 0 & 0 & 0 & 0 & 0 & 0 & 0 & 0 & 0 \\
0 & 0 & 0 & a'_2 & -a'_2 & \cdots & 0 & 0 & 0 & 0 & 0 & 0 & 0 & 0 & 0 & 0 \\
0 & 0 & 0 & 0 & 0 & \cdots & a_j & a_j & b_{j+1} & b'_{j+1} & 0 & 0 & 0 & 0 & 0 & 0 \\
0 & 0 & 0 & 0 & 0 & \cdots & a'_j & -a'_j & c_{j+1} & c'_{j+1} & 0 & 0 & 0 & 0 & 0 & 0 \\
0 & 0 & 0 & 0 & 0 & \cdots & 0 & 0 & a_{j+1} & a_{j+1} & b_{j+2} & b'_{j+2} & \cdots & 0 & 0 & 0 \\
0 & 0 & 0 & 0 & 0 & \cdots & 0 & 0 & a'_{j+1} & -a'_{j+1} & c_{j+2} & c'_{j+2} & \cdots & 0 & 0 & 0 \\
0 & 0 & 0 & 0 & 0 & \cdots & 0 & 0 & 0 & 0 & 0 & 0 & 0 & a_{n-1} & a_{n-1} & -a_n \\
0 & 0 & 0 & 0 & 0 & \cdots & 0 & 0 & 0 & 0 & 0 & 0 & 0 & a'_{n-1} & -a'_{n-1} & -a'_n
\end{vmatrix}. \quad (12)$$

In Eq. (12), we define

$$\begin{aligned}
&a_j = \chi_{\perp j}^{-1}, \quad a'_j = -\frac{\varepsilon_{zj}q_{zj}}{\chi_{\perp j}q_\perp}, \\
&b_j = -\chi_{\perp j}^{-1}e^{-q_{zj}(z_j - z_{j+1})}, \quad b'_j = -\chi_{\perp j}^{-1}e^{q_{zj}(z_j - z_{j+1})}, \\
&c_j = \frac{\varepsilon_{zj}q_{zj}}{\chi_{\perp j}q_\perp}e^{-q_{zj}(z_j - z_{j+1})}, \quad c'_j = -\frac{\varepsilon_{zj}q_{zj}}{\chi_{\perp j}q_\perp}e^{q_{zj}(z_j - z_{j+1})}.
\end{aligned} \quad (13)$$

From the Eq. (12), we can obtain the dispersion relation of single wurtzite symmetry quantum well as

$$2q_{z,0}\varepsilon_{z,0}q_{z,1}\varepsilon_{z,1} + \frac{q_{z,0}^2\varepsilon_{z,0}^2 + q_{z,1}^2\varepsilon_{z,1}^2}{q_{z,0}\varepsilon_{z,0}q_{z,1}\varepsilon_{z,1}}\tanh(q_{z,1}d_1) = 0. \quad (14)$$

In Eq. (14), we use index 1 for the quantum well material and 0 for the barrier material, d_1 is the width of the quantum well.

By using a standard quantization procedure and the relation $H_{e-ph} = -e\phi(\vec{r})$,[14] the electron-phonon interaction Hamiltonian for the interface optical phonons in wurtzite Q2D multilayer heterostructures can be obtained as follows:

$$H_{e-ph} = \sum_m \sum_{q_\perp} e^{i\vec{q}_\perp \cdot \vec{\rho}}\Gamma_m(q_\perp, z)[\hat{\alpha}_m(\vec{q}_\perp) + \hat{\alpha}_m^+(-\vec{q}_\perp)], \quad (15)$$

where $\Gamma_m(q_\perp, z)$ is electron-phonon coupling functions and is given by

$$\Gamma_m(q_\perp, z) = B_0\left(\frac{\hbar e^2}{8A\varepsilon_0\omega_m(q_\perp)}\right)^{\frac{1}{2}} \times \begin{cases} f_1(q_\perp, z), & z < z_0, \\ f_2(q_\perp, z), & z_{j-1} < z < z_j, \; j = 1,2,3 \cdots\cdots n-1, \\ f_3(q_\perp, z), & z > z_n, \end{cases} \quad (16)$$

where A is the cross-sectional area of the heterostructures, B_0 is normalization constant, and $f_i(q_\perp, z)$ $(i = 1, 2, 3)$ are defined as

$$f_1(q_\perp, z) = \alpha_{-,0}e^{q_\perp(z-z_0)} + (\alpha_{+,0} - \alpha_{-,0})e^{q_{z,0}(z-z_0)} + D_{2n-1}a_{+,n}e^{q_\perp(z-z_{n-1})} + \sum_{j=1}^{n-1}[(D_{2j}a_{-,j} - D_{2j-1}a_{+,j})e^{q_\perp(z-z_l)} - (D_{2j-1}a_{+,j}e^{q_{z,j}d_j} - D_{2j}a_{-,j}e^{-q_{z,j}d_j})e^{q_\perp(z-z_{j-1})}], \tag{17}$$

$$\begin{aligned} f_2(q_\perp, z) = {} & \alpha_{+,0}e^{q_\perp(z-z_0)} + \sum_{l=1}^{j-1}[(D_{2l}a_{+,l} - D_{2l-1}a_{-,l})e^{q_\perp d_l} + (D_{2l-1}a_{-,l}e^{q_{z,l}d_l} - D_{2l}^*a_{+,l}e^{-q_{z,l}d_l})]e^{-q_\perp(z-z_{l-1})} \\ & + (D_{2j-1}e^{-q_{z,j}(z-z_j)} + D_{2j-1}e^{q_{z,j}(z-z_j)})(a_{+,j} - a_{-,j}) + (D_{2j-1}a_{-,j}e^{q_{z,l}d_j} - D_{2j}a_{+,j}e^{-q_{z,j}d_j})e^{-q_\perp(z-z_{j-1})} \\ & + (D_{2j}a_{-,j} - D_{2j-1}a_{+,j})e^{q_\perp(z-z_j)} + \sum_{l=j+1}^{n-1}[(D_{2l}a_{-,l} - D_{2l-1}a_{+,l})e^{-q_\perp d_l} + D_{2l-1}a_{+,j}e^{q_{z,l}d_l} - D_{2j}a_{-,j}e^{-q_{z,j}d_j}]e^{q_\perp(z-z_{l-1})} \\ & + D_{2n-1}a_{+,n}e^{q_\perp(z-z_{n-1})}, \end{aligned} \tag{18}$$

$$\begin{aligned} f_3(q_\perp, z) = {} & \alpha_{+,0}e^{q_\perp(z-z_0)} + \sum_{l=1}^{n-1}[(D_{2l}a_{+,l} - D_{2l-1}a_{-,l})e^{q_\perp d_l} + D_{2l-1}a_{-,j}e^{q_{z,l}d_l} - D_{2j}a_{+,j}e^{-q_{z,j}d_j}]e^{q_\perp(z-z_{l-1})} \\ & + D_{2n-1}[e^{-q_{z,n}(z-z_{n-1})}(a_{+,n} - a_{-,n}) - a_{-,n}e^{-q_\perp(z-z_{n-1})}]. \end{aligned} \tag{19}$$

In Eqs. (17)–(19), $\alpha_{\pm,j}$ and D_j are defined as

$$a_{\pm,j} = \frac{1 \pm \gamma_j}{q_{z,j} \pm q_\perp}, \tag{20}$$

$$D_j = \begin{vmatrix} b_1 & b_1' & 0 & 0 & 0 & \ldots a_0 & \ldots 0 & 0 & 0 & 0 & 0 & 0 & 0 & 0 & 0 \\ c_1 & c_1' & 0 & 0 & 0 & \ldots a_0' & \ldots 0 & 0 & 0 & 0 & 0 & 0 & 0 & 0 & 0 \\ a_1 & a_1 & b_2 & b_2' & \ldots & \ldots 0 & \ldots 0 & 0 & 0 & 0 & 0 & 0 & 0 & 0 & 0 \\ a_1' & -a_1' & c_2 & c_2' & \ldots & \ldots 0 & \ldots 0 & 0 & 0 & 0 & 0 & 0 & 0 & 0 & 0 \\ 0 & 0 & 0 & a_2 & a_2 & \ldots 0 & \ldots 0 & 0 & 0 & 0 & 0 & 0 & 0 & 0 & 0 \\ 0 & 0 & 0 & a_2' & -a_2' & \ldots 0 & \ldots 0 & 0 & 0 & 0 & 0 & 0 & 0 & 0 & 0 \\ 0 & 0 & 0 & 0 & 0 & \ldots 0 & \ldots a_j & a_j & b_{j+1} & b_{j+1}' & 0 & 0 & 0 & 0 & 0 \\ 0 & 0 & 0 & 0 & 0 & \ldots 0 & \ldots a_j' & -a_j' & c_{j+1} & c_{j+1}' & 0 & 0 & 0 & 0 & 0 \\ 0 & 0 & 0 & 0 & 0 & \ldots 0 & \ldots 0 & 0 & 0 & 0 & 0 & 0 & a_{n-1} & a_{n-1} & -a_n \end{vmatrix}. \tag{21}$$

D_j is $2n \times 2n$ determinant. It should be noticed that the jth column in D_j was substituted by the column matrix $(a_0, a_0', 0, 0, \ldots 0, 0)$.

III. NUMERICAL RESULTS AND DISCUSSION

Based on our theory given in Sec. II, we have calculated the effect of ternary mixed crystals on interface optical phonons in single $In_xGa_{1-x}N$/GaN QW. The corresponding experimental data are listed in Table I.

Figure 2 is a plot for phonon energies for ternary crystal $In_xGa_{1-x}N$ and binary GaN. The results show that A_1 (LO), A_1 (TO), E_1 (LO), and E_1 (TO) phonons indicate one-mode behavior.[13] There are eight optical phonon branches in $In_xGa_{1-x}N$, the upper four branches are strong modes, which take (+) sign in Eq. (1), and the lower four branches are weak modes, which take (–) sign in Eq. (1). The strong modes have been reported in experiment; the weak modes have not yet been reported experimentally.[15] The results

TABLE I. Optical phonon energies (in meV), dielectric constants, effective charge (in e_0), and other parameters in caculations.

Material	$\omega_{z,T}$	$\omega_{\perp,T}$	$\omega_{z,L}$	$\omega_{\perp,L}$	$\varepsilon_{\infty,z}$	$\varepsilon_{\perp,z}$	e_z	$e_\perp$	a	c
GaN	65.91[a]	69.25[a]	90.97[a]	91.83[a]	6.38[b]	6.11[b]	2.86b	2.69[b]	3.20[b]	5.22[b]
InN	55.27[c]	58.87[c]	70.14[c]	73.45[b]	7.96[b]	7.61[b]	2.96[b]	2.78[b]	3.48[b]	5.64[b]

[a]Reference 13.
[b]Reference 15.
[c]Reference 16.

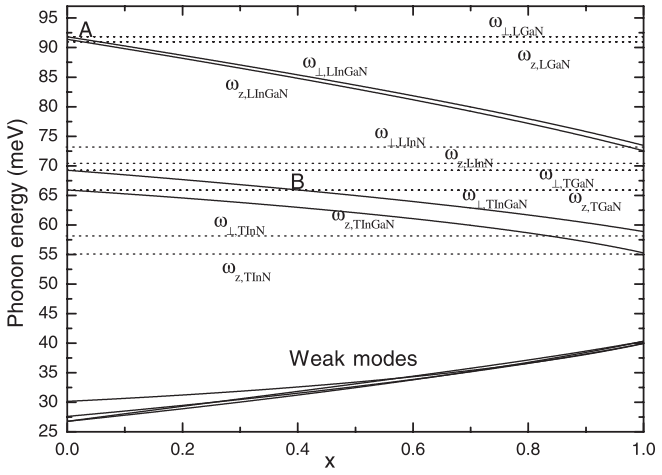

FIG. 2. Optical phonon energies of E_1(LO), A_1(LO), E_1(TO), and A_1(TO) branches for $In_xGa_{1-x}N$ as a function of indium composition x. Lower four curves below 40 meV are the weak modes of E_1 and A_1.

show that A_1 (LO), A_1 (TO), E_1 (LO), and E_1 (TO) phonons indicate one-mode behavior. In this paper, we only consider the strong modes. From our calculation, we can see that the frequencies of optical phonons (A_1 and E_1) vary almost linearly with compositional indium changes, which has been verified by ultraviolet Raman study.[16] With the increase of indium composition (x), the phonons curves of ternary crystal $In_xGa_{1-x}N$ and binary GaN intersect two points ($x_A = 0.05, x_B = 0.40$). From the frequencies of optical phonons A_1 (LO), A_1 (TO), E_1 (LO), and E_1 (TO) in ternary crystal $In_xGa_{1-x}N$ and binary GaN, some authors[17] have gave out their frequency ranges of five distinct types of optical-phonon modes. In this paper, we only pay attention to the interface optical phonons.

The effect of the concentration (x) of indium on the dispersions of interface optical phonons is plotted in Fig. 3. Numerical calculations show that two branches of interface optical phonons appear in high frequency range $(\omega_{\perp,L1}, \omega_{z,L2})$ when the indium concentration (x) is in the range (0.05, 0.40). When x is in the range (0.40, 1.00), four branches of interface optical phonons appear in high frequency range $(\omega_{\perp,L1}, \omega_{z,L2})$ and low frequency range $(\omega_{\perp,T1}, \omega_{z,T2})$. We can observe that the frequencies of interface optical phonons are almost linearly with increasing indium concentration when indium concentration is smaller than 0.25 (see Fig. 3(b)). But in high indium concentration range ($x \geq 0.25$), the frequencies of interface optical phonons do not vary almost linearly with compositional changes (x) (see Fig. 3(a)). So the empirical formula[18] cannot been used to investigate all kinds of phonon modes in wurtzite quantum wells. From Fig. 3 we can see that the behavior of interface optical phonons in $In_xGa_{1-x}N$/GaN quantum well is different from that in InN/GaN or GaN/AlN quantum well,[4,8] where exist four branches of interface optical phonon in high frequency range $(\omega_{\perp,L1}, \omega_{z,L2})$ and low frequency range $(\omega_{\perp,T1}, \omega_{z,T2})$. Which is similar to those in $In_xGa_{1-x}N$/GaN quantum well when indium concentration x is in the range (0.40, 1.00).[19] But when x is in the range (0.05, 0.40), only two branches of interface optical phonon appear in high frequency range $(\omega_{\perp,L1}, \omega_{z,L2})$. Therefore, the behaviors of the interface optical phonon in

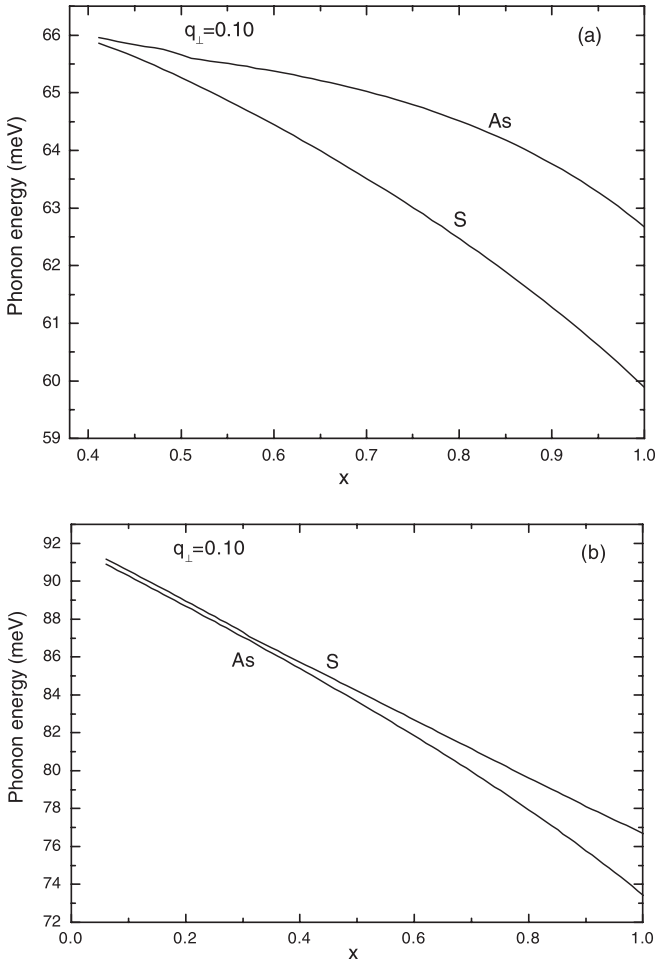

FIG. 3. The effect of indium composition (x) on dispersion curves of interface optical phonons for an $In_xGa_{1-x}N$ QW of width d = 5 nm sandwiched between two semi-infinite GaN barrier layers ($q_\perp = 0.10$). Here (a) for the interface optical phonon in low frequency range $(\omega_{\perp,T1}, \omega_{z,T2})$, and (b) for the interface optical phonon in high frequency range $(\omega_{\perp,L1}, \omega_{z,L2})$.

$In_xGa_{1-x}N$/GaN QW are strongly dependent on the indium concentration.

The effect of the concentration (x) of indium on the electron-phonon interaction of interface optical phonons is plotted in Fig. 4. We can observe that the electron-phonon interactions for symmetric modes in low frequency range $(\omega_{\perp,T1}, \omega_{z,T2})$ increase, and reach a maximum ($x = 0.86$), then decrease linearly with the increase of indium concentration (x). For the anti-symmetric modes in low frequency range $(\omega_{\perp,T1}, \omega_{z,T2})$, electron-phonon interactions decrease with the increase of indium concentration (x), and almost reach the same value when $x \geq 0.7$ (see Fig. 4(a)). From Fig. 4, we can also see that the electron-phonon interactions for interface optical phonons in high frequency range $(\omega_{\perp,L1}, \omega_{z,L2})$ increase nonlinearly with the increase of concentration (x) of indium, reach a maximum (x = 0.27), then decrease nonlinearly with the increase of concentration (x) of indium (see Fig. 4(a)). Comparing the electron-phonon interactions in the two frequency ranges, we can conclude that the electron-phonon interactions in the low frequency range are stronger than that in the high frequency range.

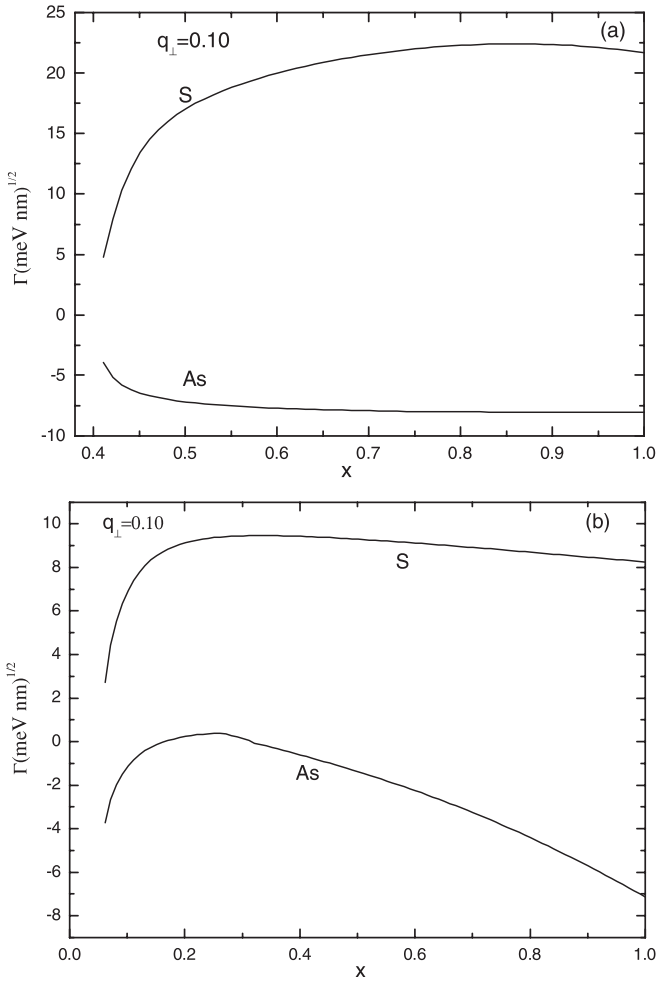

FIG. 4. The effect of indium composition (x) on electron-phonon coupling functions $\Gamma(q_\perp, z)$ for the interface optical phonons in the same QW as in Fig. 3 ($q_\perp = 0.10$). Here (a) for the interface optical phonon in low frequency range $(\omega_{\perp,T1}, \omega_{z,T2})$, and (b) for for the interface optical phonon in high frequency range $(\omega_{\perp,L1}, \omega_{z,L2})$.

IV. CONCLUSION

Within the framework of the modified random-element isodisplacement model and DC model, we have studied the interface optical phonons and electron-phonon interaction in wurtizte $In_xGa_{1-x}N$/GaN QWs. When the indium concentration (x) is in the range (0.05, 0.40), the IO phonons appear in high frequency range. With the increase of the indium concentration (x), the electron-IO phonon interactions for symmetric mode increase, and reach a maximum, then decrease linearly. For the anti-symmetric modes, their electron-phonon interactions decrease linearly. When x is in the range (0.40, 1.00), the interface optical phonons appear in high frequency range and low frequency range. With the increase of the indium concentration (x), the electron-phonon interactions in low frequency range decrease linearly. For the interface optical phonons in high frequency range, the symmetric modes are non-linear increase, and the anti-symmetric modes are non-linear decrease.

These results and conclusions are important and useful for further experimental and theoretical investigations of phonon effect in arbitrary wurtzite Q2D multilayer heterostructures, such as the polaron effect, the bound polaron effect, and the exciton-phonon interaction.

ACKNOWLEDGMENTS

This work was supported by the National Natural Science Foundation of China (Grant Nos. 61176079 and 51106093), Scientific Research Program Funded by Shaanxi Provincial Education Department (Grant No.12JK0982), and Natural Science Basic Research Plan in Shaanxi Province of China (Grant Nos. 2011JM1016 and 2009JM1012).

[1]S. Nakamura and G. Fasol, *The Blue Laser Diodes: GaN Light Emitters and Lasers* (Springer, Berlin, 1997).
[2]J. Li, K. B. Nam, K. H. Kim, J. Y. Lin, and H. X. Jiang, Appl. Phys. Lett. **78**, 61 (2001).
[3]H. Hirayama, A. Kinoshita, T. Yamabi, Y. Enomoto, A. Hirata, T. Araki, Y. Nanishi, and Y. Aoyagi, Appl. Phys. Lett. **80**, 207 (2002).
[4]D. Romanov, V. Mitin, and M. Stroscio, Phys. Rev. B **66**, 115321 (2002).
[5]S. M. Komirenko, K. W. Kim, and M. A. Stroscio, Phys. Rev. B **59**, 5013 (1999).
[6]B. C. Lee, K. W. Kim, M. A. Stroscio, and M. Dutta, Phys. Rev. B **58**, 4860 (1998).
[7]J. Gleize, M. A. Renucci, J. Frandon, and F. Demangeot, Phys. Rev. B **60**, 15985 (1999).
[8]J. J. Shi, Phys. Rev. B **68**, 165335 (2003).
[9]J. J. Shi and X. L. Chu, Phys. Rev. B **70**, 115318 (2004).
[10]J. T. Lü and J. C. Cao, Phys. Rev. B **71**, 155304 (2005).
[11]S. Y. Wei, Y. Wang, and L. L. Wei, Phys. B **405**, 272 (2010).
[12]Z. W. Zhou and H. J. Xie, Phys. Lett. A **375**, 2007 (2011).
[13]S. Yu, K. W. Kim, L. Bergman, L Bergman, M. Dutta, and M. A. Stroscio, Phys. Rev. B **58**, 15283 (1998).
[14]L. Wendler and R. Haupt, Phys. Status Solidi B **143**, 487 (1987).
[15]D. Behr, R. Niebuhr, J. Wagner, K. H. Bachem and U. Kaufmann, in *Galliun and Related Materials II*, edited by C. R. Abernathy, H. Amano, and J. C. Zolper (Materials Research Society, Pittsburgh, 1997), p. 213.
[16]D. Alexson, L. Bergman, R. J. Nemanich, M. Dutta, M. A. Stroscio, C. A. Parker, S. M. Bedair, N. A. El-Masry, and F. Adar, J. Appl. Phys. **89**, 798 (2001).
[17]Y. Qu and S. L. Ban, Acta. Phys. Sin. **59**, 4863–4873 (2010).
[18]A. Kasic, M. Schubert, J. Off *et al.*, Phys. Status Solidi C **0**, 1750–1759 (2003).
[19]J. H. Zhu, J. Q. Ning, C. C. Zheng, S. J. Xu, S. M. Zhang, and H. Yang, Appl. Phys. Lett. **99**, 113115 (2011).